引用格式：LONG Hu，CHEN Hong-yi，LU Xiao-wei，*et al*. Filtering Characteristics of an MIM Waveguide Filter Based on a Rectangular Cavity[J]. *Acta Photonica Sinica*，2020，**49**(2)：0223001
龙虎，陈红艺，陆小微，等.一种基于矩形腔的 MIM 波导滤波器的滤波特性研究[J].光子学报，2020，**49**(2)：0223001

一种基于矩形腔的 MIM 波导滤波器的滤波特性研究

龙虎[1,2]，陈红艺[1]，陆小微[1]，蔡懿[1]，曾选科[1]，李景镇[1]
（1 深圳大学 电子科学与技术学院 深圳市微纳光子信息技术重点实验室，广东 深圳 518060）
（2 深圳大学 光电工程学院 光电子器件与系统(教育部/广东省)重点实验室，广东 深圳 518060）

摘 要：理论提出并研究了一种基于矩形腔的窄带金属-介质-金属波导滤波器.建立滤波器内电场的传递矩阵模型，研究了矩形微腔与直通波导间耦合特性对器件滤波特性的影响.同时，研究了耦合长度、矩形微腔腔长、传输损耗等因素对滤波带宽的影响.研究结果表明，对于不同的矩形微腔腔长，存在一个可使器件滤波带宽达到最窄的耦合系数.此外，当微腔腔长越长且传输损耗越小时，滤波带宽也将越窄.该研究为表面等离子体波导的研究与设计提供了一定的参考.

关键词：表面等离子体；金属-介质-金属；波导滤波器；微腔；传递矩阵
中图分类号：TN252 **文献标识码**：A **doi**：10.3788/gzxb20204902.0223001

Filtering Characteristics of an MIM Waveguide Filter Based on a Rectangular Cavity

LONG Hu[1,2], CHEN Hong-yi[1], LU Xiao-wei[1], CAI Yi[1], ZENG Xuan-ke[1], LI Jing-zhen[1]
(1 *Shenzhen Key Laboratory of Micro-Nano Photonic Information Technology, College of Electronic Science and Technology, Shenzhen University, Shenzhen, Guangdong* 518060, *China*)
(2 *Key Laboratory of Optoelectronic Devices and System of Ministry of Education and Guangdong Province, College of Optoelectronic Engineering, Shenzhen University, Shenzhen, Guangdong* 518060, *China*)

Abstract: A narrow-band Metal-Insulator-Metal (MIM) waveguide filter based on a rectangular cavity is proposed and investigated in theory. The influences of the coupling characteristics between the microcavity and the waveguide on the filtering characteristics, which have not been clearly demonstrated before, are studied by establishing a transfer matrix theoretical model for the transmission of electric fields in the filter. The effects of coupling length, rectangular cavity length, and propagation loss on the filtering bandwidth are also analyzed. It is found that for different resonance cavity lengths, there is an optimal coupling coefficient at which the filtering bandwidth is the narrowest. In addition, the greater the resonance cavity length and the lower the cavity loss, the narrower the filter bandwidth. These would provide some reference for the research and development of surface plasmon polariton filters.

Key words: Surface plasmon polarition; Metal-insulator-metal; Waveguide filter; Microcavity; Transfer

Foundation item: The National Major Scientific Instruments and Equipments Development Project of National Natural Science Foundation of China (No. 61827815)

First author: LONG Hu (1986—), male, postdoctor, Ph.D. degree, mainly focuses on SPP waveguide devices, fiber laser and amplifier technology. Email:lhu@szu.edu.cn

Corresponding author: LI Jing-zhen (1940—), male, professor, M.S. degree, mainly focuses on high-speed photography and transient optical imaging. Email:lijz@szu.edu.cn

Received: Sep.15, 2019; **Accepted**: Nov.14, 2019

matrix

OCIS Codes: 230.3120; 230.7408; 240.6680; 260.3160

0 Introduction

Surface Plasmon Polaritons (SPP) are electromagnetic waves coupled to electron oscillations and propagating at the interface between an insulator and a conductor[1]. Because the fields of SPP decay exponentially in both sides, SPP can overcome the conventional diffraction limit and manipulate light on a subwavelength scale. Therefore, SPP have promising applications in highly integrated optical circuits[2-3]. Several SPP waveguiding structures have been proposed and studied, such as V-groove waveguides[4], dielectric-loaded waveguides[5], long-range waveguides[6], and Metal-Insulator-Metal (MIM) waveguides[7], to propagate and control SPP effectively. Among these structures, MIM waveguide can focus the light into the insulator core and allow the manipulation and propagation of light at the nanoscale. Hence, MIM waveguide has attracted tremendous interests of researchers in recent years, and various devices based on SPP have been proposed and demonstrated theoretically and experimentally, such as beam splitters[8], couplers[9], Mach-Zehnder interferometers[10], and filters[11-14].

MIM waveguide filters are essential components in SPP integrated circuits. Kinds of filters with filtering bandwidth ranging from tens to hundreds of nanometers based on resonance interference effect have been proposed, including the T-shape structure[13], ring cavity structure[14], Fabry-Perot structure[15], and rectangle cavity structure[16-17]. The effects of cavity structure parameters on the resonance peak and extinction ratio have been studied as well. Since the easy fabrication, the MIM waveguide filters based on microcavity structure have been well-studied. However, filtering bandwidth of those filters is generally wide, that is difficult to meet the requirements of narrow-bandwidth application. Moreover, in fact, the filtering characteristics of microcavity structure filters are based on the coupling between the microcavity and the waveguide, which shows that the coupling will affect the filtering bandwidth of the filter indeed. Unfortunately, there is no relevant research on this aspect at present.

In this study, an MIM waveguide filter based on a rectangular cavity is constructed, and the filtering characteristics of this type of filter are studied. First, a transfer matrix theoretical model for the transmission of electric fields in the filteris established. The effects of the coupling length, rectangular cavity length, and propagation loss on the filtering bandwidth are studied and analyzed. Finally, the narrow 3-dB filtering bandwidth of the filter is obtained by optimizing the coupling length and the rectangular cavity length with loss compensation with the introduction of a gain medium. This work may provide some reference for the research and development of SPP filters.

1 Theoretical model

Fig.1 shows the structure of the MIM waveguide SPP filter. The filter is made of a straight MIM waveguide and a rectangular cavity-based MIM waveguide. The reason for choosing rectangular cavity as resonance microcavity is that on the one hand, it is convenient to change the coupling length between cavity and straight waveguide to study the influence of coupling effects on filtering characteristics. On the other hand, the structure of rectangular cavity is simple and easy to manufacture. The width (d) of both

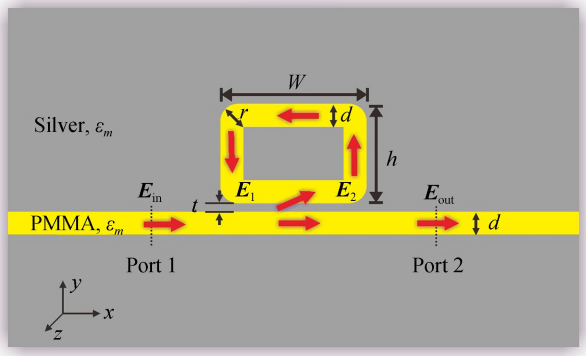

Fig.1 Structure of the MIM waveguide filter

the waveguides is 50 nm. The metal used in the waveguides is silver, and the intermediate insulator layer is poly (methyl methacrylate) (PMMA). The relative permittivities of the silver and PMMA are ε_m and $\varepsilon_d = 2.25$, respectively. ε_m can be obtained from the Drude model[17]

$$\varepsilon_m(\omega) = \varepsilon_\infty - \omega_p^2/(\omega^2 + \mathrm{i}\omega\gamma) \tag{1}$$

Here, $\varepsilon_\infty = 3.7$ is the interband transition contribution, ω is the angular frequency, $\omega_p = 1.38 \times 10^{16}$ Hz is the plasmon oscillation frequency of the free electrons in the metal, and $\gamma = 2.7 \times 10^{13}$ Hz is the damped oscillation frequency. W and h denote the outside width and height of the rectangular cavity, respectively. The distance (t) between the rectangular cavity and the waveguide is 10 nm. To reduce the propagation loss of the SPP in the rectangular cavity and improve the Q value of the cavity, we used a rectangular cavity with a smooth bend structure on the outer portion[18]. The radius (r) of the arc is 50 nm. When the initial SPP (the electric field is E_{in}) are incident at Port 1 of the straight waveguide, a portion of the energy is directly outputted from Port 2 (the electric field is $\boldsymbol{E}_{\mathrm{out}}$), and the remaining portion (the electric field is $\boldsymbol{E}_2$) is transmitted counterclockwise after being coupled to the rectangular cavity via the coupling region with a length of W. After being transmitted for a length of $L_1 = [(W-d)+(h-d)] \times 2$, the SPP (the electric field is $\boldsymbol{E}_1$) in the rectangular cavity interfere with the incident SPP through the coupling region. According to the principle of the transfer matrix theory[19], a theoretical model for the transmission of electric fields in the MIM waveguide filter can be built. The electric field $\boldsymbol{E}_{\mathrm{out}}$ can be expressed as follows

$$\begin{bmatrix} \boldsymbol{E}_{\mathrm{out}} \\ \boldsymbol{E}_2 \end{bmatrix} = \begin{bmatrix} \sqrt{\tau} & \mathrm{i}\sqrt{\kappa} \\ \mathrm{i}\sqrt{\kappa} & \sqrt{\tau} \end{bmatrix} \begin{bmatrix} \boldsymbol{E}_{\mathrm{in}} \\ \boldsymbol{E}_1 \end{bmatrix} \tag{2}$$

where κ is the coupling coefficient of the coupling region, and τ is the transmission coefficient. $\kappa + \tau < 1$ because of the existence of loss in the coupling region. According to the Maxwell equations, $\boldsymbol{E}_1$ and $\boldsymbol{E}_2$ should satisfy the following relationship

$$\boldsymbol{E}_1 = \boldsymbol{E}_2 \exp(-\mathrm{i}\beta L_1) \tag{3}$$

Here, β is the propagation constant of the SPP mode in the MIM waveguide. According to Eq (2) and (3), the transmittance of the filter can be expressed as follows

$$T = \frac{\boldsymbol{E}_{\mathrm{out}}}{\boldsymbol{E}_{\mathrm{in}}} \left(\frac{\boldsymbol{E}_{\mathrm{out}}}{\boldsymbol{E}_{\mathrm{in}}} \right)^* \tag{4}$$

The propagation constant β can be calculated from the dispersion relationship[13]

$$\tanh\left(\frac{1}{2} \mathrm{d}k_1 \right) = -\frac{\varepsilon_d k_m}{\varepsilon_m k_d} \tag{5}$$

where $k_d = \sqrt{\beta^2 - \varepsilon_d k_0^2}$ and $k_m = \sqrt{\beta^2 - \varepsilon_m k_0^2}$ are the longitudinal propagation constants of the dielectric and metal, respectively. $k_0 = 2\pi/\lambda$ is the propagation constant in vacuum, and λ is the wavelength. Eqs (2)~(5) are the models for the propagation of electric fields in the MIM waveguide filter. They show that the transmissivity is related to the transmission length, coupling splitting ratio, loss, and propagation constant. The transmissivity properties of the device are then studied and analyzed by conducting a numerical simulation.

2 Results and discussions

We first calculated the propagation constant of the SPP mode in the MIM waveguide. Without loss of generality, we assume that the wavelength is 1 550 nm and that the waveguide supports only one SPP mode with a propagation constant $\beta = (8.26 \times 10^6 + 2.5 \times 10^4 \mathrm{i})\ \mathrm{m}^{-1}$, which is calculated using Eq (5). We conducted a numerical simulation and analysis combined with a finite element method (FEM) to investigate the properties of the coupling region[9]. Fig.2(a) shows the variation in the coupling coefficient κ and transmission coefficient τ with the coupling length W. τ tends to decrease first and then increase periodically with the increase in W. However, the trend is the opposite for κ. Moreover, $\kappa + \tau < 1$, and the sum value keeps decreasing with the increase in the coupling length, indicating an increase in the loss. On this basis, we studied the influences of the height h of the rectangular cavity on the filtering characteristics. For $W = 300$ nm, Fig.2(b) shows the trend in the filter transmissivity for different height h of the rectangular cavity simulated using the established theoretical model; the results simulated using the

FEM are also included.

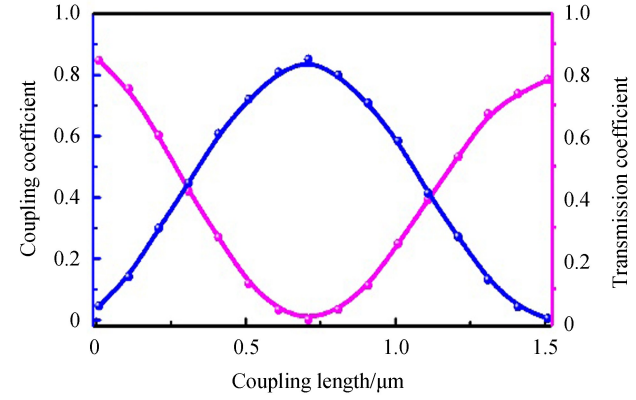

(a) Variation of the coupling coefficient κ and transmission coefficient τ over the coupling length W

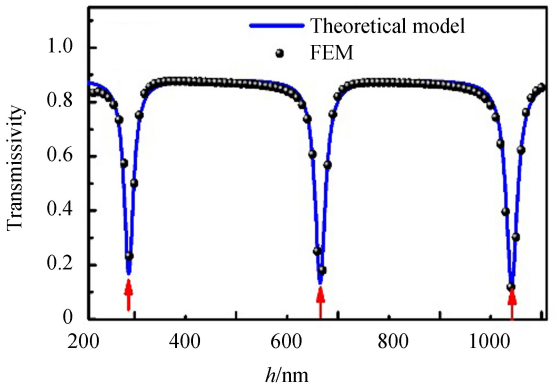

(b) Variation in the transmissivity of the filter with the h

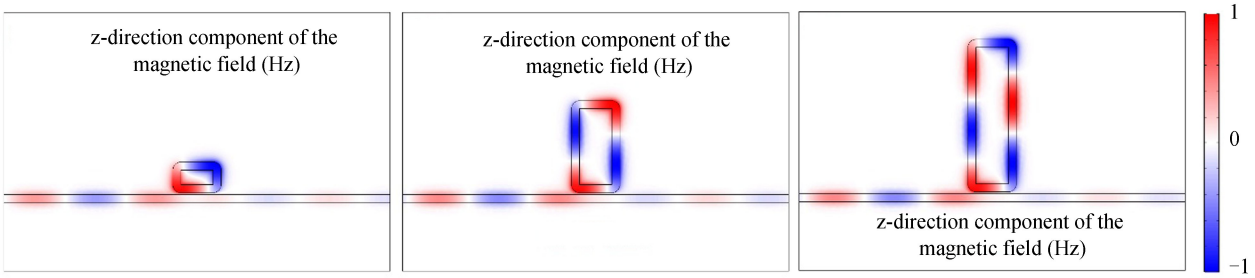

(c) h=190 nm (d) h=570 nm (e) h=950 nm

Fig.2 Characteristics of the filter varying with the h

The figure shows that with the increase in h from 100 to 1 000 nm, three filtering drop peaks are observed at h=190, 570, and 950 nm, and the corresponding transmissivity values are 0.23, 0.18, and 0.12, respectively. This indicates that 1 550 nm SPP achieve resonance in the cavity at the three heights. To clearly show the resonance characteristics, we give the distribution of the z-direction component of the magnetic field ($\boldsymbol{H}_z$) simulated using the FEM for h=190, 570, and 950 nm, as shown in Figs.2(c)～(e). For h=190 nm, the length of the rectangular cavity is equal to the wavelength of the SPP mode, as shown in Fig.2(c), and this satisfies the conditions of constructive interference. For h=570 and 950 nm, the transmission length is increased by 760 nm, and the length of one wavelength of the SPP mode is added at the same time (as shown in Figs.2(d) and (e)). With the propagation constant β, the SPP wavelength λ_{SPP} is found to be 760 nm ($2\pi/\beta_R$), and β_R is the real part of the propagation constant, which is equal to the increased transmission length. The results obtained using the two theoretical methods are highly consistent, thus demonstrating the accuracy of the proposed model.

The coupling length significantly influences the filtering characteristics, particularly the filtering bandwidth. The sum of h and W is fixed at 870 nm, which corresponds to a total propagation length L_1 of 1 540 nm in the rectangular cavity and ensures the length of twice SPP wavelengths (as shown in Fig.2(d)). The variation in the transmissivity spectrum with the coupling length W is studied, as shown in Fig.3. The transmissivity spectrum of the filter is different for different W. With the increase in W from 200 to 550 nm, the 3 dB filtering bandwidth narrows first and then widens. When W is equal to 250 nm (κ equals 0.36), the transmissivity spectrum has the narrowest filtering bandwidth of 40 nm and an extinction ratio of 23 dB (as shown in Fig.3(b)); when W equals 400 nm (κ equals 0.6), although the extinction ratio is as high as 36 dB, the filtering bandwidth reaches 100 nm (as shown in Fig.3(d)); when W is greater than 500 nm, the filtering bandwidth and extinction ratio decrease to a very low level, and the resonance peak wavelength shifts to the longer wavelength region (Figs.3(e)～(f)). This shows that although the coupling coefficient increases gradually with the increase in W, there is an optimal coupling length at which the narrowest filter bandwidth can be achieved. This phenomenon could be the result of the combined influence of the coupling coefficient and loss. In the case of resonance, when the cavity loss is approximately equal to the coupling coefficient, the electric field coupled to the waveguide and the incident

electric field in the waveguide can interfere perfectly with each other, and the bandwidth is the narrowest (Fig.3 (b)). When the cavity loss is less than or greater than the coupling coefficient, the transmittance increases and the filter bandwidth widens.

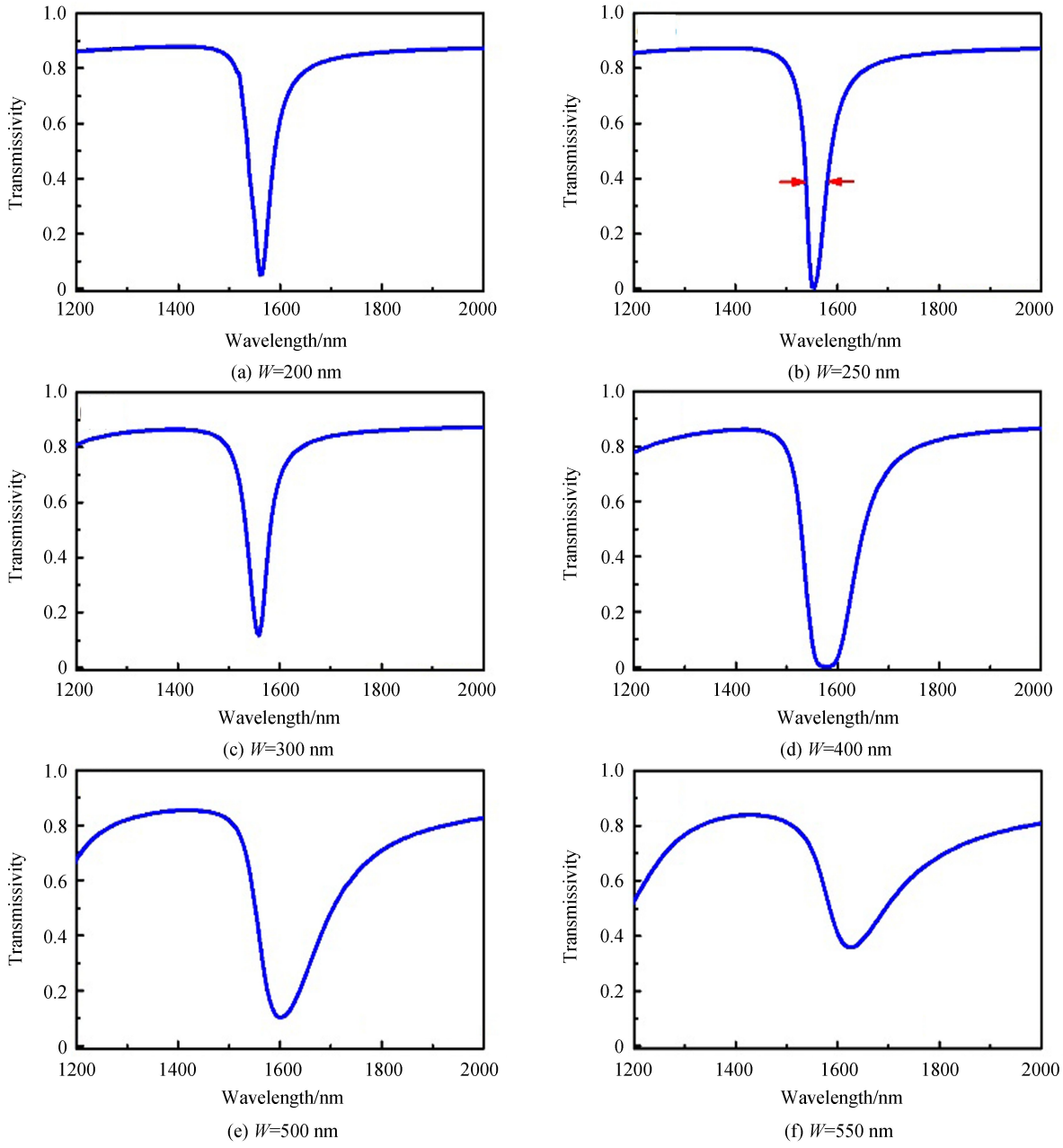

Fig.3 Variation of transmissivity spectrum with different coupling lengths W when L_1 is 1 540 nm

We studied the filtering characteristics of the filter in cases when the propagation length L_1 is equal to one and three times the SPP wavelength, as shown in Figs.2(c) and 2(e). The sums of h and W were fixed at 490 and 1 250 nm, and the propagation lengths were 780 and 2 300 nm, respectively. We investigated the transmissivity spectra for $L_1=780$ and 2 300 nm for different W. The results show that for different L_1, the narrowest filtering bandwidth is achieved when $W=250$ nm, as shown in Fig.4(a). For $L_1=780$ nm, the filtering bandwidth is 70 nm, and the extinction ratio is 20 dB, whereas for $L_1=2\ 300$ nm, the filtering bandwidth is only 30 nm, and the extinction ratio is 25 dB. Therefore, the filtering bandwidth of the filter decreases gradually with the increase in the resonance length of the rectangular cavity, and the coupling length corresponding to the narrowest filter bandwidth remains unchanged. Fig.4(b) shows the distribution of the absolute value of the electric field ($|E|$) in the filter for a wavelength of 1 550 nm when the narrowest filtering bandwidth is achieved at resonance lengths of 780, 1 540, and 2 300 nm. The figure

shows that the filter realizes a high extinction ratio filtering at 1 550 nm for the three structural parameters.

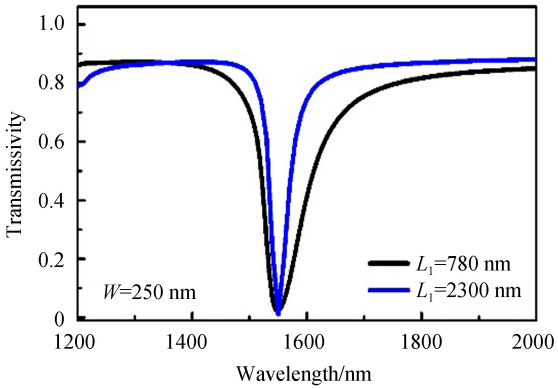

(a) Transmissivity spectra of the filter for L_1=780 nm and 2300 nm when W=250 nm

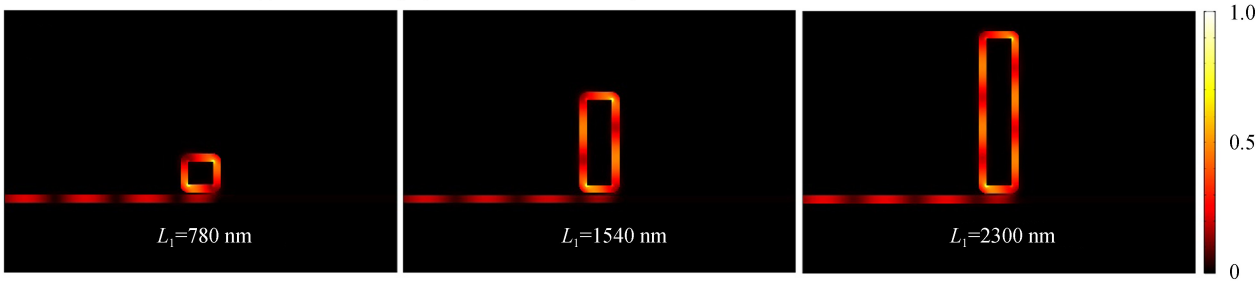

(b) Distribution of the absolute value of the electric field ($|\boldsymbol{E}|$) for L_1=780 nm, 1540 nm and 2300 nm when W=250 nm

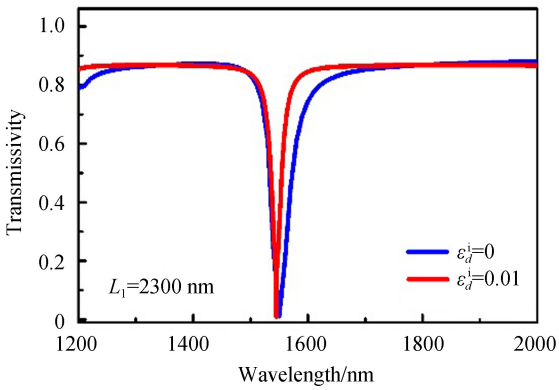

(c) Transmissivity spectra of filter before and after the introduction of gain medium in the intermediate insulator layer when L_1=2300 nm and W=250 nm

Fig.4 Transmissivity spectra and electric field of the filter

The previous analysis showed that in addition to the coupling coefficient κ, the propagation loss of the SPP in the rectangular cavity affects the filtering bandwidth of the device. To further realize a filter with a narrower filtering bandwidth, we introduced an optical gain medium to compensate for the propagation loss. Lead sulfide (PbS) quantum dots were used as the gain medium for the 1 550 nm SPP[20]. They were doped into the PMMA material at the intermediate layer of the rectangular cavity. As such, the PbS quantum dots provided gain for the SPP under the external pumping light, thus overcoming the problem of wide filtering bandwidth due to excessive cavity loss. Fig.4(c) shows the transmissivity spectra of the filter before and after the introduction of the PbS quantum dots as the gain medium when L_1 = 2 300 nm and W = 250 nm. We assume that the dielectric constant of the PMMA changes from a real number ε_d = 2.25 to a complex number ε_d = 2.25 + 0.01 · i (the imaginary part is ε_d^i = 0.01) when the gain medium is introduced. The figure shows that as the cavity loss could be partially compensated by introducing the gain medium, the filtering bandwidth becomes narrower, i.e., from 30 to 15 nm. This indicates that the filtering bandwidth of the filter based on the cavity can be further narrowed down by introducing a gain medium.

3 Conclusion

The filtering characteristics of an MIM waveguide filter based on a rectangular cavity are investigated in this study. A transfer matrix theoretical model for the transmission of electric fields in the filter is established, and the effects of the coupling length, rectangular cavity length, and propagation loss on the filtering bandwidth are analyzed. The simulation results indicate that for different resonance cavity lengths, there is an optimal coupling coefficient at which the filtering bandwidth is the narrowest. Moreover, the greater the resonance cavity length and the lower the cavity loss, the narrower the filter bandwidth. For an optimum coupling length of 250 nm and a rectangular cavity length of 2 300 nm, the 3 dB filtering bandwidth of the MIM waveguide filter is found to be 30 nm at a wavelength of 1 550 nm. The filtering bandwidth can be narrowed down to 15 nm by introducing PbS quantum dots as the gain medium into the rectangular cavity to compensate for the propagation loss. This paper may provide some reference for the research and development of SPP filters.

References

[1] BARNES W L, DEREUX A, EBBESEN T W. Surface plasmon subwavelength optics[J]. *Journal of Beijing Technology & Business University*, 2003, **424**(6950): 824-830.

[2] LEZEC H J. Beaming light from a subwavelength aperture[J]. *Science*, 2002, **297**(5582): 820-822.

[3] MAIER S A. Plasmonics: the promise of highly integrated optical devices[J]. *IEEE Journal of Selected Topics in Quantum Electronics*, 2007, **12**(6): 1671-1677.

[4] PILE D F P, GRAMOTNEV D K. Plasmonic sub wavelength waveguides: Next to zero losses at sharp bends[J]. *Optics Letters*, 2005, **30**(10): 1186-1188.

[5] BO Y, YE L, MAO Q. Investigations of influences of spontaneous emission properties onsurface plasmonpolariton amplifications with the rate-equation theory[J].*Journal of the Optical Society of America B*, 2015, **32**(11): 2326.

[6] OULTON R F, SORGER V J, GENOV DA, *et al*. A hybrid plasmonic waveguide for subwavelength confinement and long-range propagation[J]. *Nature Photonics*, 2008, **2**(8): 496-500.

[7] LIU L, HAN Z, HE S. Novel surface plasmon waveguide for high integration[J].*Optics Express*, 2005, **13**(17): 6645.

[8] HWANG Y, KIM J E, PARK H Y. Frequency selective metal-insulator-metal splitters for surface plasmons[J].*Optics Communications*, 2011, **284**(19): 4778-4781.

[9] HAN Z, LIU L, FORSBERG E. Ultra-compact directional couplers and Mach-Zehnder interferometers employing surface plasmon polaritons[J]. *Optics Communications*, 2006, **259**(2): 690-695.

[10] PU M, YAO N, HU C, *et al*. Directional coupler and nonlinear Mach-Zehnder interferometer based on metal-insulator-metal plasmonic waveguide[J]. *Optics Express*, 2010, **18**(20): 21030-21037.

[11] MING T, PING L, LI C, *et al*. Plasmonic Bragg reflectors based on metal-embedded MIM structure[J]. *Optics Communications*, 2012, **285**(24): 5122-5127.

[12] DAVOODI F, GRANPAYEH N. Nonlinear manipulation of surface plasmons on graphene-TMDC Bragg reflectors[J]. *Optical and Quantum Electronics*, 2019, **51**(1): 9.

[13] LIN X S, HUANG X G. Tooth-shaped plasmonic waveguide filters with nanometeric sizes.[J].*Optics Letters*, 2009, **33**(23): 2874-2876.

[14] ZHENG G, SU W, CHEN Y, *et al*. Band-stop filters based on a coupled circular ring metal-insulator-metal resonator containing nonlinear material[J]. *Journal of Optics*, 2012, **14**(5): 651-658.

[15] YUN B, HU G, CUI Y. A nanometric plasmonic waveguide filter based on Fabry - Perot resonator[J]. *Optics Communications*, 2011, **284**(1): 485-489.

[16] HOSSEINI A, MASSOUD Y. Nanoscale surface plasmon based resonator using rectangular geometry[J]. *Applied Physics Letters*, 2007, **90**(18): 10484.

[17] ARIANFARD H. Tunable band (pass and stop) filters based on plasmonicstructures using Kerr-type nonlinear rectangular nanocavity[J]. *Optical Engineering*, 2016, **56**(12): 121902.

[18] TIAN M, LU P, CHEN L, *et al*. A subwavelength MIM waveguide resonator with an outer portion smooth bend structure[J].*Optics Communications*, 2011, **284**(16): 4078-4081.

[19] MORTIMORE D B. Fiber loop reflectors[J].*Journal of Lightwave Technology*, 1988, **6**(7): 1217-1224.

[20] RADKO I, NIELSEN M G, ALBREKTSEN O, *et al*. Stimulated emission of surface plasmon polaritons by lead-sulphide quantum dots at near infra-red wavelengths[J]. *Optics Express*, 2010, **18**(18): 18633.